Experimental method for the determination of the under-stress first-plasticization process parameters

A. Risitano, G. Fargione
Department of Industrial Engineering, University of Catania, Catania (Italy)
arisitan@diim.unict.it

ABSTRACT. Uniaxial static traction tests and fatigue tests, performed on smooth and notched specimens of C40 steel have confirmed that starting from the thermal analysis of the specimen under test it is possible to evaluate the fatigue limit of the material.

Further, starting from post processing image analysis, the parameters that characterize the dynamic behavior of the material have been characterized; in particular in the case of notched specimen.

Test results have shown that utilizing adequate sensors it is possible to make estimations very close to the real values of both the stress concentration factor and the fatigue-stress concentration factor. It is possible therefore to distinguish between the total elastic behavior and the partial elastic behavior that is the behavior characterized by some irreversible deformation of specific microarea of the material.

The experimental results proposed in the present paper, have outlined the possibility to define some parameters related to the total deformation density energy. Those parameters can be determined also in the cases of local plasticization that usually does not allow to provide immediate and verified measurements.

SOMMARIO. Le prove statiche di trazione e di fatica eseguite su provini lisci ed intagliati ad U di acciaio C40 hanno confermato che attraverso l'analisi termica della superficie del provino durante le prove è possibile valutare il limite di fatica del materiale. Ad ulteriore conferma sono stati anche stimati, attraverso post-processing delle immagini termiche acquisite durante le prove, i parametri che caratterizzano il comportamento dinamico del componente ed in particolare, nel caso specifico, del provino con intaglio. I risultati delle prove hanno evidenziato che lavorando con adeguati sensori è possibile fare delle stime molto prossime a quelli teorici del fattore di forma (stress concentration factor) e del fattore di effetto di intaglio (fatigue-stress concentration factor) potendo distinguere in modo preciso il comportamento *totalmente elastico* dal comportamento parzialmente elastico ovvero in cui in qualche microarea del materiale è iniziato il processo di deformazione irreversibile. La sperimentazione eseguita nel presente lavoro ha evidenziato fra l'altro la possibilità di definire parametri legati alla densità di energia totale di deformazione anche in quei casi in cui il processo di locale plasticizzazione non ne permette immediate e sicure quantificazioni.

KEYWORDS. Fatigue; Stress concentration; Plasticity; Thermal analysis.

INTRODUCTION

T he energy dissipated as heat in a specimen during fatigue tests of material was proposed as fatigue damage index by many researchers [1-11]. But in the actual literature are few the authors that analyze the specimen during static tests [12, 13]. It is seen that by analyzing the surface temperature of the specimen during the static traction tests, see [14-17], it is possible to estimate the fatigue limit of the material.

The study of the fatigue resistance of mechanical components needs the evaluation of parameters that depends on the geometry and characteristics of the material under test [18-26].

In mechanical components the definition of the fatigue-stress concentration factor is a problem difficult to evaluate quantitatively. It is known that it is related both to the stress concentration factor, function of the specimen geometry, and to the characteristic of the material via the notch sensitivity factor.

The stress concentration factor and the fatigue-stress concentration, that in some cases can be easily determined, became uncertain when the shape of the component is complicated and the material has not been appropriately characterized. In this case just some numerical methods can be applied [27, 28].

In the simple cases the fatigue-stress concentration factor can be evaluated as the ratio between the fatigue limits of the smooth and notched specimens of the same material.

This approach can be easily followed in the laboratories by using specimens. It becomes difficult to apply for mechanical components because they are generally difficult to test for fatigue in long run and for which high power machines are necessary.

In literature, see [29, 36], are available theoretical models that allow to evaluate the equivalent deformation at break energy also in specimens with sever notch, for which the concentration effect of the tension brings to local condition outside the perfect elastic filed.

By analyzing the surface temperature during the static traction tests, see [14-17], it is possible to evaluate characteristic parameters of the material or the notched specimens that usually are computed theoretically or via fatigues tests.

The identification of the perfect elastic areas and the areas where irreversible deformations begin during the load application, becomes very important for the evaluation of parameters like the Equivalent Strain Energy Density (ESED) or other parameters linked to this kind of transformation.

AIM OF THE WORK

Starting from the authors previous experience on the surface temperature analysis, the paper aims to determine the fatigue-stress concentration factor (linked with local plasticization effects) starting from experimental measurement of the thermal release of the apex of the notch (also acute) in specimens under static traction load. In the meanwhile it is adopted the methodology proposed in [15] but applied to different material and different shapes. In particular the fatigue limit is estimated identifying the end of the total elastic phase taking into account that in any point of the material , in this phase, also at microscopic level, the process of plasticization is not already started. During this phase, it applies the provisions of the thermoelastic theory [37], that implies a perfect linearity between stress and temperature. In this case of total perfect elasticity, as is known, for different notched cases, there are analytical expressions of the stresses [18] that permit to calculate energetic parameters as the ESED [29, 30] or as a isothermal map [37].

A behavior of the material non totally elastic, can be detected also for stress whose value is lower than the classical yield limit $\sigma_{0.2}$ and often close to the fatigue limit of the material (σ_0 for R=-1). Therefore in our definition, out to the total elastic field and also at microscopic level and for deformation values lower than the yield limit, it starts local plasticization phenomena or irreversible deformation with heat production.

Post processing thermal images, acquired during the application of static traction load on the specimen surface, are utilized to analyze the relation between the stresses and the temperature variation on the entire surface with particular attention to notch areas. A thermal stress concentration factor α_{iT} is estimated and consequently the value of β_{iT}, linked to the notch sensitivity, is valuated. The value of fatigue-stress concentration factor β_t is computed starting from the stress concentration factor α_t [38]. It is evaluated the ratio β_{ts} of the fatigue limits of smooth and notched specimens. It is estimated β_{tst} as ratio between σ corresponding T_0 for material base and T_0 for notched specimens, being T_0 the temperature corresponding to the end of the total thermo-elastic phase (determined via static tests). It is outlined that the data obtained after the image post processing allow to analyze the behavior of the material also in the zone between the fatigue limit at oscillating stress σ_0 and the yield limit $\sigma_{0.2}$. The analysis of this zone has been not enough investigated.

ADOPTED PROCEDURE

In order to confirm the obtained results and taking into account the novelty of the proposed approach, a lot of confirmatory tests have been performed applying also traditional methodologies.
It follows the test procedure flow:

1. Static characterization of the material by using smooth specimens and surface thermal image acquisition;
2. Static characterization of notched specimens and surface thermal image acquisition;
3. For smooth specimens determination of the fatigue limit and Wöhler curve by applying Risitano Rapid Method [4, 5];
4. For notched specimens determination of the fatigue limit and Wöhler curve by applying Risitano Rapid Method;
5. Check of the fatigue limits by applying the traditional approach (two specimens stressed with the parameters previously obtained);
6. Determination of the coefficient of notch effect (β_{is}) as ratio between the fatigue limits of smooth and notched specimens;
7. Image post processing of the two type of specimens (#1 and #2) to determine the reference zone (maximum temperatures);
8. Evaluation of the temperature variation on the surface of the specimens during the phase of perfect thermo-elastic behavior (temperature vs deformation perfectly linear and stress values under the fatigue limit);
9. Definition of the ratios of maximum and medium (nominal) temperature in the perfect thermo-elastic behaviour (α_{iT});
10. Evaluation of T_0 for smooth and notched specimens, estimation of the fatigue limits and evaluation of their ratio β_{tst};
11. Comparison of the parameters α_i reported in literature with α_{iT};
12. Definition of the notch effect coefficient (β_i) via the sensitivity notch factor η;
13. Evaluation of the specimens surface temperature variation during the thermo-plastic phase (temperature vs deformation out the linear zone and tension values over the fatigue limit);
14. Definition of the ratios of maximum and medium (nominal) temperature in the perfect thermo-plastic behavior (β_{iT});
15. Comparison among the notch effect coefficients: theoretical β_i, experimental (β_{is}, β_{iT}, β_{tst}) ;

In the paper, due to the large number of performed tests, it has been preferred to report only the essential ones so to provide specific information on the adopted procedure that represents a test protocol.

TEST MODE

It is premise that for each type of test (static or dynamic) three specimens have been utilized. In the following the results related just to one test per type are given and not the mean value of the three tests. This choice it to reduce the space for tests report and because the results for the three specimens are almost coincident. Due to the novelty of the proposed approach the authors preferred to report the images as they are without any filtering for image enhancing.

The adopted specimens are of C40 steel. The chemical characteristics of C40 steel are reported in Tab. 1. In Tab. 2 are given the mechanical characteristics. Tests have been performed with an electro-hydraulic machine INSTRON 8501, with a load of 100KN. During all the tests the surface temperature of specimens was continuously stored. For the thermal image acquisition it has been adopted a FLIR-3000 system. The FLIR-3000 consists of a infrared thermo camera, pc for data acquisition and post processing and the ThermaCAM Researcher tool operating in Windows environment. The thermal parameters of the system are given in Tab. 3. The fatigue tests have been performed applying to the specimens an oscillating load and therefore a load ratio $R = \sigma_i/\sigma_s = -1$ at the frequency of 10Hz. The surface temperature of the specimen has been detected with the thermal camera and analyzed with the previously introduced software at fixed frequency. For the fatigue tests the sampling frequency was fixed to 10s and test frequency (10Hz).

C [%]	Mn [%]	Si [%]	P [%]$_{max}$	S [%]$_{max}$
0.400	0.500	0.400	0.045	0.045

Table 1: Chemical composition of the C 40 steel.

E [MPa]	$\sigma_{0,2}$ [MPa]	σ_u [MPa]
206000	540	890

Table 2: Mechanical characteristics of the C 40 steel.

Scanning Frequency	Temperature Range [°C]	Thermal Resolution [°C]
1 image to 10 seconds	10 ÷ 150	0.02

Table 3: Characteristics of the thermal system.

All the specimens are black painted and their thermal emission coefficient was close to 0.92. Fig. 2 shows on broken specimen. For the static characterization of the material (#1 of the procedure) three specimens with shape and dimension showed in Fig. 1 have been utilized (D= 12.5mm; d= 11.36 mm; s= 5 mm). For each specimen a classic traction test with fixed constant values of the load velocity [N/s] has been performed. Also in this case, during the test, the surface temperature of the specimen has been stored. The same test have been performed on three U notched specimens (r= 2.84 mm; α_i= 1.6) as reported in Fig. 1 (#2 of the procedure). Also in this case thermal image of the specimen surface have been acquired.
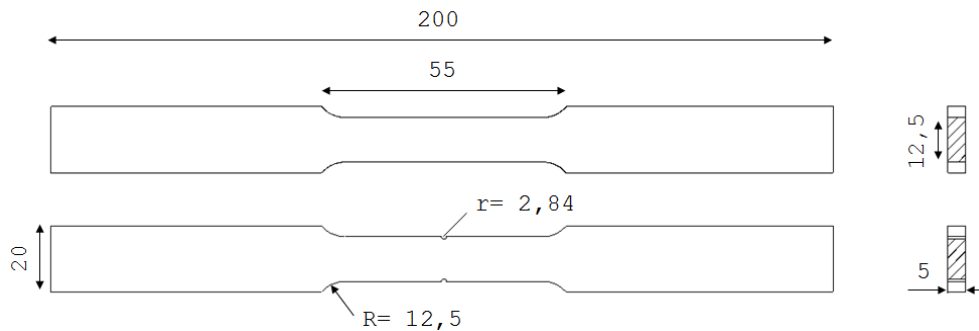
Figure 1: Geometrical properties of the specimens [mm].

Figure 2: Painted, smooth and broken specimen.

Once the specimens broke the acquired images have been analyzed backwards starting from the thermal image at the broke time to determine the area of the specimen at higher temperature. With this approach the curve time vs load and consequently time vs temperature have been determined. In the static tests the load velocity [N/s] is equal to 120 N/s. For the notched specimens the temperature in three points (named A, B and C) have been analyzed. The point A is close to the notch, the point B is in the half of the notch section and the point C is far from the notch in a point not affected by the presence of the notch itself (Fig. 3). Fig. 4 shows the temperature vs time for one of the three specimens utilized for the static characterization of the material (not notched specimens). Fig. 5 shows the temperature vs time for one of the three specimens utilized for the static characterization of the notched specimens.

For the fatigue characterization, by using three smooth specimens (not notched, base material), dynamic tests with step loads (Fig. 6) have been performed applying the Risitano Rapid Method [4, 5]. This procedure allows to determine the material limit of fatigue (#3 of the procedure). Fig. 7 shows, for one specimen, the temperature curve vs the number of cycles for each value of the applied load. The same procedure has been applied on the same number of notched

specimens (# 4 of the procedure) to determine their fatigue limit. Fig. 9 shows the temperature vs the number of cycles for the various steps of applied load.
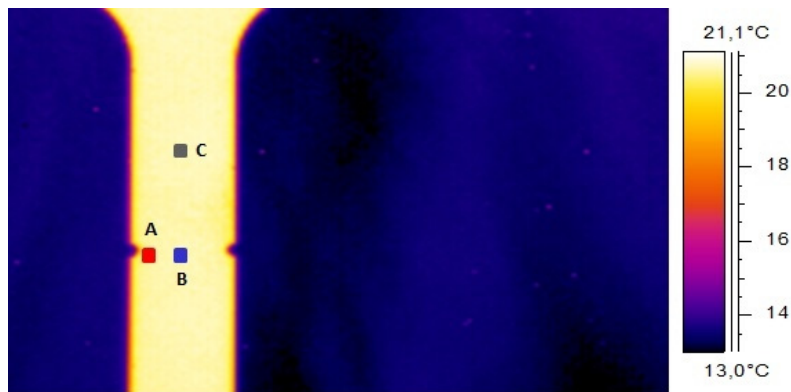
Figure 3: Points on the surface of notched specimens chosen for analysis of the temperatures.
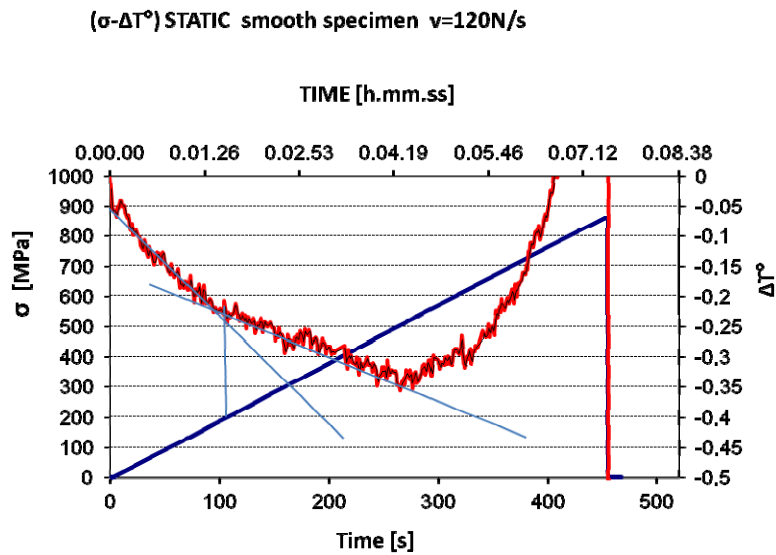
Figure 4: Temperature vs Time (applied load) for smooth specimens.
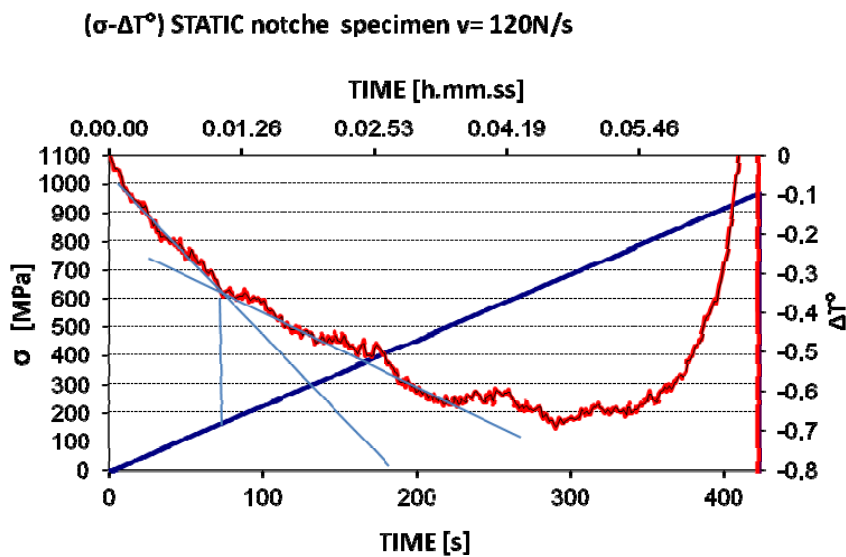
Figure 5: Temperature vs Time (applied load) for the notched specimens.

Load/Time
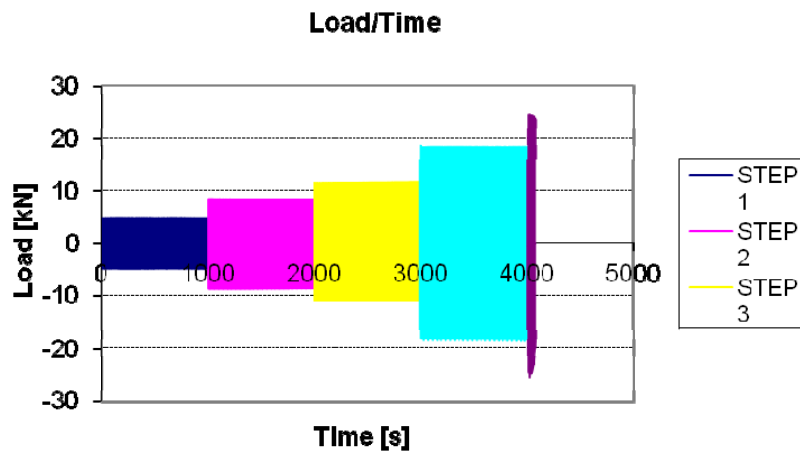
Figure 6: Load vs Time (load frequency *f*= 10Hz) for fatigue tests.

The data provided in Fig. 7 and 9 allowed to determine the fatigue limits, with the procedure given in [4, 5] for the two cases: base material and notched specimens. The diagrams of Fig. 8 and 10 synthesize as reported in [4, 5].
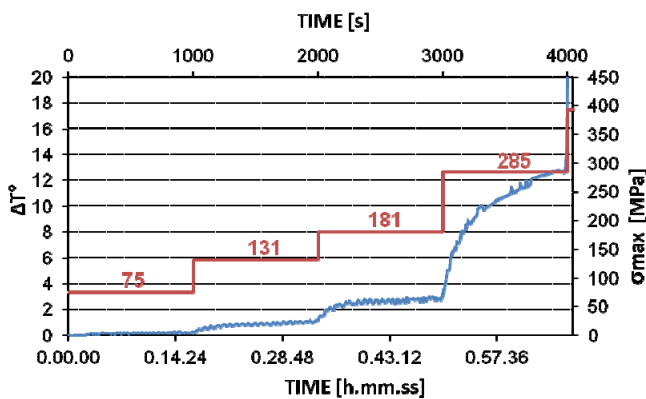
Figure 7: Temperature vs Time for applied step load to the smooth specimens.
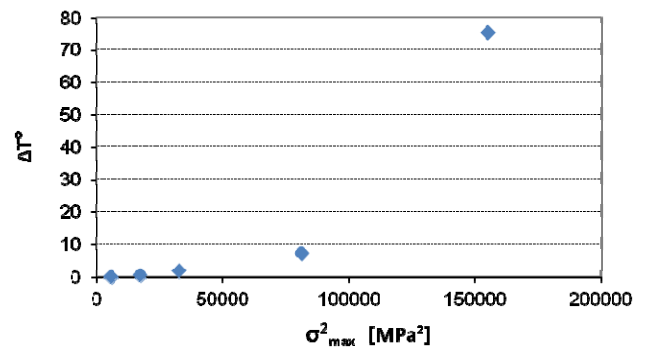
Figure 8: Temperature vs σ^2 for smooth specimens.
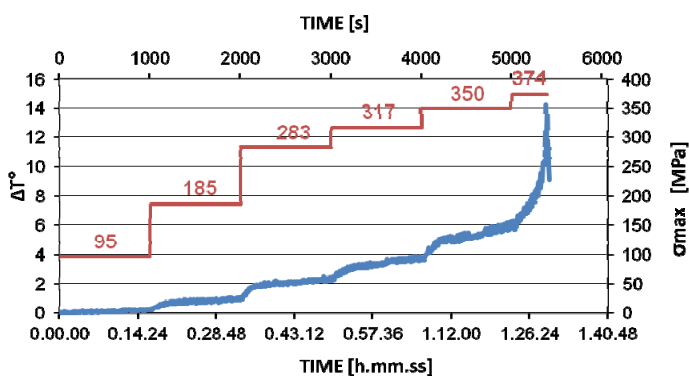
Figure 9: Temperature vs Time for applied step load to the notched specimens.
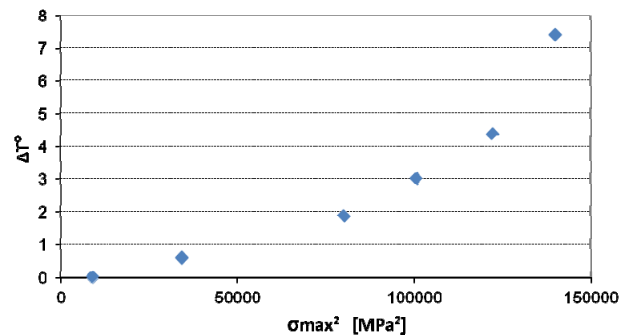
Figure 10: Temperature vs σ^2 for notched specimens.

From the data showed in Fig. 9 and 10 it is possible to deduce that the fatigue limit for the base material can be estimated in 220 MPa and in 165 MPa for the notched specimens with a ratio β_{is} equal to 1.33. The value of the fatigue limit is equal

to that reported in the diagram of Fig. 11 computed with the traditional method as in [39]. For further confirmation two specimen of base material have been tested between 200 MPa and 210 MPa. After 2 milion cycles the specimens didn't shown any break (# 5 of the procedure). In the diagram of Fig. 11 of Berto and Lazzarin [39] the results by traditional tests are also reported. In this case it has been adopted a specimen with a "V" notch, a radius of 0.5 mm and therefore more severe of that applied in our case (Fig. 1). It is possible to note that the value of the fatigue limit for the specimens of [39] is close to the values for the notched specimens that we tested. This is justified by the actual strong influence of geometry on the results of fatigue in the presence of notches.
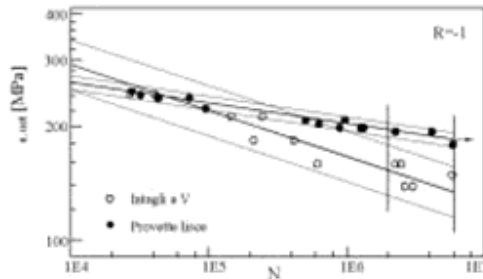
Figure 11: Fatigue curve for C40 steel as in literature [39].

TESTS RESULTS AND ANALYSIS

The results of the dynamic tests (#1 to #5 of the procedure) allowed to obtain the fatigue limit of the material and the notched specimens that are equally respectively to 220 MPa and 165 MPa. The ratio of the two values for each specimen provided a notched effect coefficient β_{is}= 1.33 (#6 of the procedure). Starting from data available in literature [18, 38], the geometrical aspect (*D*= 12.5 mm; *d*= 11.36 mm; *r*= 2.84 mm) (*r/d*= 0.25; *D/d*=1.1; a_i= 1.6) and the material characteristic ($\sigma_r \approx 870$ MPa) $\eta = 0.80$, it resulted a theoretical coefficient β_i= 1 + η (α_i -1)= 1.48.

Once the value of β_{is} has been determined the thermal curves related to the static tests both for the base material and notched specimens have been analyzed (# 7 of the procedure). The total elastic behavior field of the material has been defined that is the field from load 0 to the load out of the perfect linear law between temperature and stress. As it is known in this field the relation between stress and load is proportional.

For three specimens of base material and three specimens of notched material the curves that links the temperature and time have been determined (#8 of the procedure). Fig. 12 and 13 show the temperature in A, B, and C (Fig. 3) for the notched specimens. It was verified that the temperature curve of the C point was very closed (practically coincident) to the temperature curve of the smooth specimens. In the Fig. 13 it has been reported the particular of Fig. 12 and the straight lines that outline the slope change. It is worth noting that the origin does not result always well defined for the recovery of the machine clearances corresponding to the start of the test. From the Fig. it is possible to estimate the stress for which the first change of slope in the two types of specimens starts.
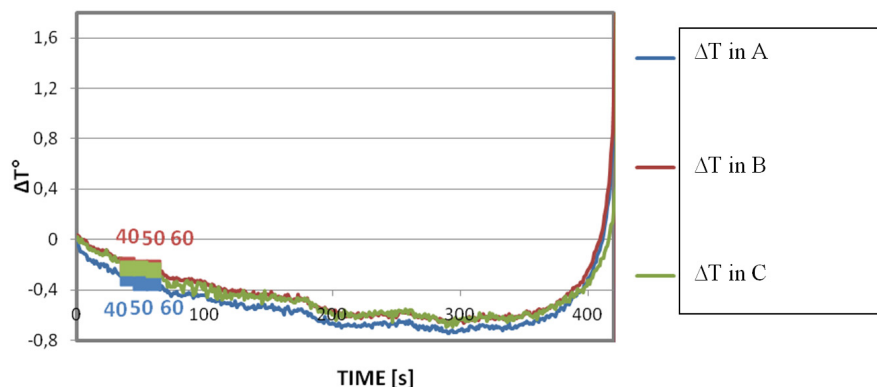
Figure 12: Temperature vs time in three different points of the notched specimens (load applied).
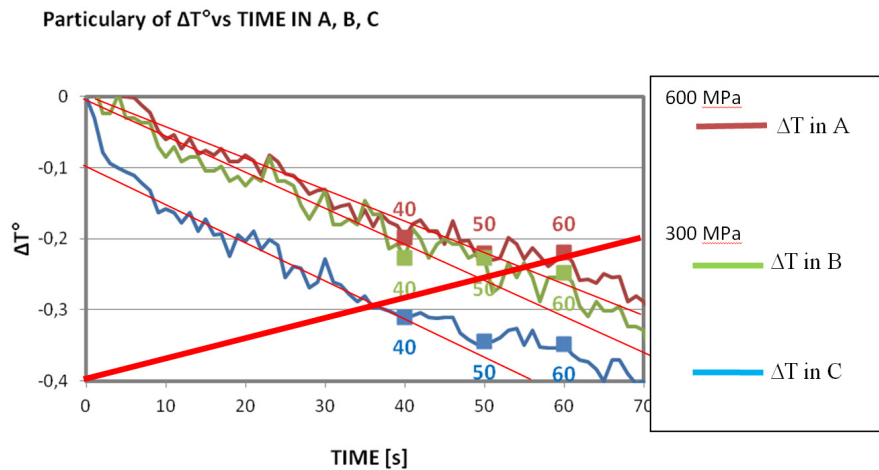
Figure 13: Particular of the temperature in the notched specimens in the *fully elastic* phase.

This stress is approximately equal to 200 MPa for the smooth specimens and approximately 160 MPa for the notched specimens with a ratio equal to 1.25. For the series of notched specimens the temperature of three points (named A, B and C in Fig. 3) have been monitored.

For one of three specimens under test, in Fig. 12, the temperature trend while the applied load (120N/s) increase is depicted. Also in this case the behavior of the three specimens is practically the same. In the figure the zone of the time at which the slope change is estimated are outlined (second).

A first analysis of the data reported in Fig. 12 shows a temperature trend that after a perfect linear phase goes flat to increase at the end of the test. This is coherent with the reaching of plasticity condition that while the load increase more larger areas are affected. The value of the temperature measured in the point C have been compared with those in the smooth specimens. It has been verified that in these points the temperature values coincide. Fig. 13, a zoom of Fig. 12, shows the three medium straight lines. It is possible to note for all the straight lines a linear trend with a different slope change for each of the three curves. The part at constant slope is more longer for the points B and C with respect to A. For the point A, due to the intensification of the stress, the local plasticity conditions are reached before. The curves for a period of 40 s keep a straight line trend and a temperature ratio (α_{iT}), for the same applied load, close to 1,54 (#9 of the procedure). This value is very similar to the stress intensification factor α_i that, as previously outlined is equal to 1,6 (#10 of the procedure). The value of (α_{iT}), defined starting from the data of Fig. 12 and 13, allowed to estimate β_{iT}=1.43 (#11 of the procedure) being for the considered steel η=0.8.

Temperatures trend in Fig. 12 show that out of the total elastic area it appears a flattening of the temperature values (smaller *ΔT*). This corresponds to the increasingly large areas of plasticization with the same value of the temperature for load values close to the break. Considering the temperature in the points A and B, for load values out of the total elastic area and after 100 s, it is possible to note that the values of β_{iT} remains constant and equal to 1.35 (#12 and #13 of the procedure). This ratio becomes 1 (the same temperature) for stress values over 800 MPa that appears in an advanced plastic phase close to the fracture stress of the material (950MPa).

In summary, the data obtained after the image post processing, allowed to define:

- α_{iT}= 1.54 as the ratio between the temperature close to the edge of the notch and the temperature far to the influence of the notch, while working in the perfect elastic phase;
- β_{is}= 1.33 as the ratio of the fatigue limits between the base material and the notched specimens, determined with the Risitano Rapid Method;
- β_{ist}= 1.25 as the ratio of the fatigue limits between the base material and the notched specimens, determined via static tests;
- β_{iT}= 1.35 as the ratio between the temperature close to the edge of the notch and the temperature far to the influence of the notch, while working outside the perfect elastic phase;
- β_i= 1.43 as fatigue-stress concentration factor computed via Peterson diagrams.

The values are reassumed in Tab. 4.

Fig. 14-22 show the temperature trend along the restricted section for different values of the applied load. In the same Fig. the trends of the theoretical axial stress along the section are reported. Fig. 14 refers to a stress equal to 109.00 MPa

lower than the specimens fatigue limit equal to 160 MPa. The ratio between the temperature close to notch and the temperature in the middle point of the specimen is equal to 0.46/0.29= 1.58.

α_i	β_i	α_{iT}	β_{is}	β_{ist}	β_{iT}
1.60	1.48	1.54	1.33	1.25	1.35

Table 4: Values of the parameters

Fig. 15-22 refer to the stresses outside of the area of totally elastic behavior for which the process of plasticization is started and the ratio between the temperature close to notch and the temperature in the middle point is equal to 1.30.
Close to the break, see Fig. 21, the temperature inverted the sign becoming positive and practically constant on the entire section of the notch. This points out the complete plasticization of the considered area. It should be noted that, according to [15], the stress values corresponding to the end of the totally elastic phase coincide (within the limits of the experiment) to the values of the fatigue limit for the given specimen obtained in the traditional way and on the basis of energy considerations (Risitano Rapid Method).

Figure 14: Temperature and axial stress along the narrow section of the specimen at 108.51 MPa.
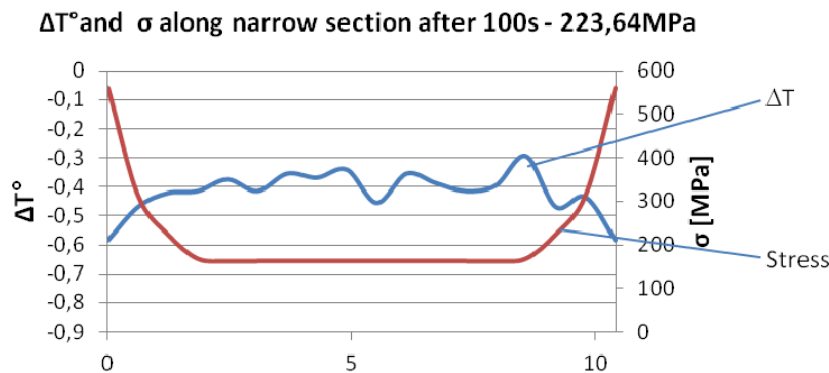
Figure 15: Temperature and stress along the narrow section of the specimen at 223.64 MPa.
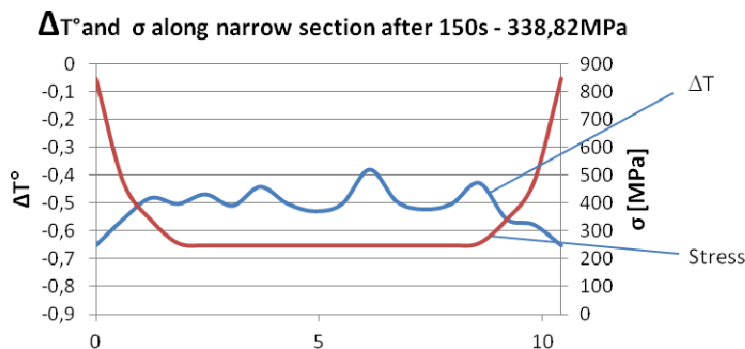
Figure 16: Temperature and stress along the narrow section of the specimen at 338.82 MPa.

ΔT°and σ along narrow section after 200s - 454,05MPa
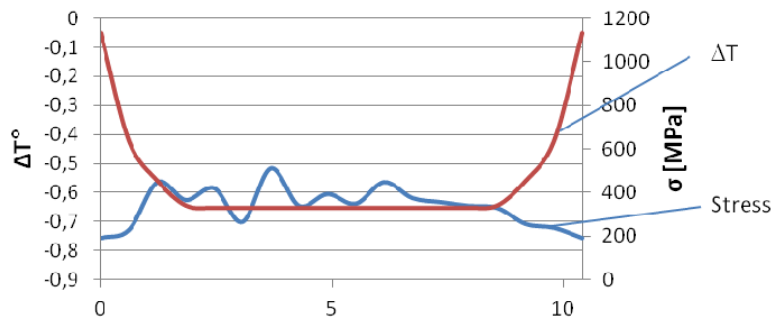
Figure 17: Temperature and stress along the narrow section of the specimen at 454.05 MPa.

ΔT°and σ along narrow section after 250s - 569,19MPa
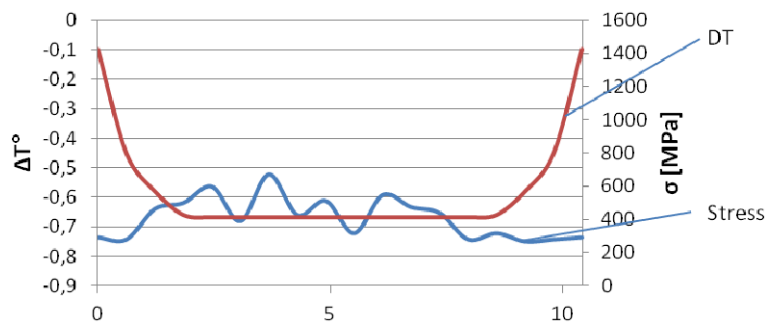
Figure 18: Temperature and stress along the narrow section of the specimen at 569.19 MPa.

ΔT°and σ along narrow section after 300s - 684,39MPa
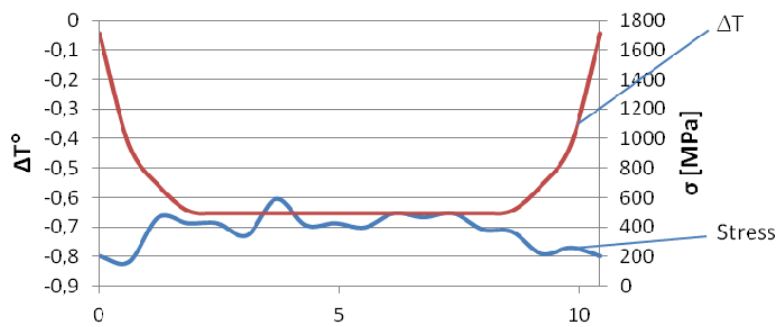
Figure 19: Temperature and stress along the narrow section of the specimen at 684.39 MPa.

ΔT°and σ along narrow section after 350s - 799,46MPa
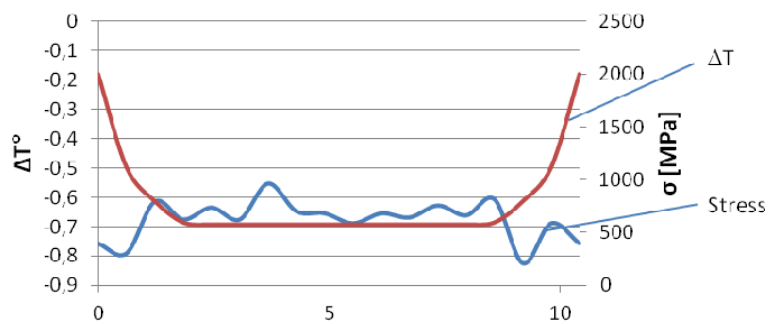
Figure 20: Temperature and stress along the narrow section of the specimen at 799.46 MPa.

ΔT°and σ along narrow section after 400s - 914,67MPa
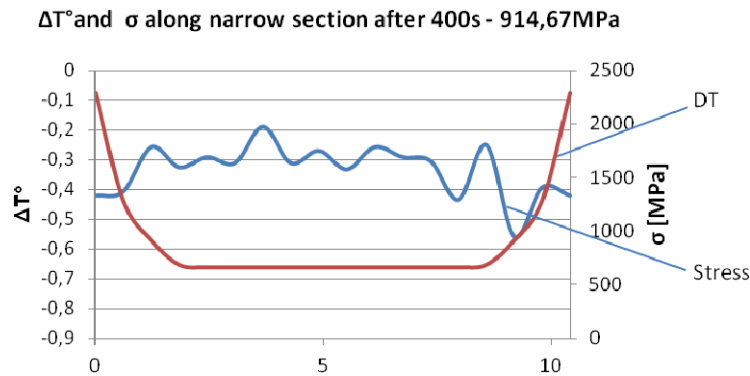
Figure 21: Temperature and stress along the narrow section of the specimen at 914.67 MPa.

ΔT°and σ along narrow section after 422s - 966,1MPa
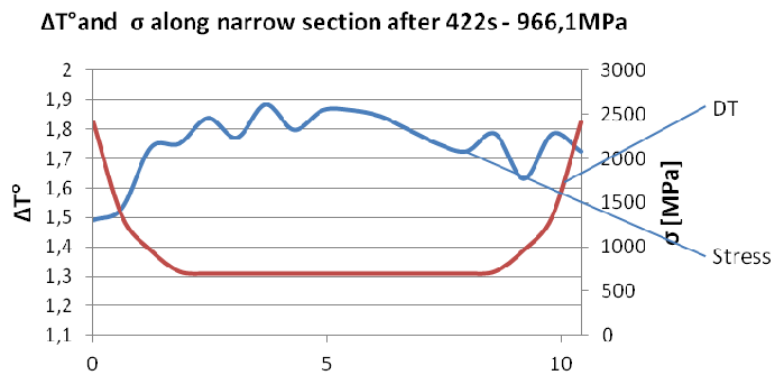
Figure 22: Temperature and stress along the narrow section of the specimen at 966.01 MPa.

CONCLUSIONS

U niaxial static traction and fatigue tests on smooth and notched specimens of steel C40 have been carried out. During the tests the surface temperature of the specimens have been acquired and successively analyzed.

It was confirmed that it is possible, by performing static traction tests, to estimate the fatigue limit on the basis of the loss of proportionality between stress and temperature. It was estimated the stress concentration factor by using the temperature of the notch apex and the temperature of the area that are not affected by the boundary form.

Starting from the thermal analysis and the stress concentration factor given in literature, the value of the fatigue-stress concentration factor has been determined by using the notch sensitivity coefficient. It was verified that the value of the fatigue-stress concentration factor practically coincides with the ratio between the fatigue limit of smooth specimens and notched specimens.

The analysis of the temperatures close the notch section, outside the perfectly elastic area, permitted to evaluate the value of the ratio between the temperature on the edge and centerline of the notch, value that remained almost constant for the whole duration of the test.

The values of the temperatures are reversed only in the vicinity of the breaking stress, (the specimen is heated instead of cooling) and the ratio is close to 1 (fully plastic section). The temperature maps close the notch has also highlighted the possibility of estimating the released thermal energy [11, 40, 41]. The comparison with the total energy density of deformation at the peak of the notch, determined according to the theoretical criteria that the current literature proposes, will be the subject of future works.

REFERENCES

[1]   D. Dengel, H. Harig, Fatigue Fract. Eng. Mater. Struct. 3 (1980) 113.

[2] G. Curti, A. Geraci, A. Risitano, Ingegneria Automotoristica, 42 (1989) 634.
[3] M. P. Luong, Nuc. Eng. Des. 158 (1995) 363.
[4] G. La Rosa, A. Risitano, Int. J. Fatigue 22 (2000) 65.
[5] G. Fargione, A. Geraci, G. La Rosa, A. Risitano, Int. J. Fatigue 24 (2002) 11.
[6] G. Meneghetti, M. Ricotta, B. Atzori, Fatigue Fract. Eng. Mater. Struct., (2013) on-line, doi: 10.111/ffe.12071.
[7] G. Meneghetti, Int. J. Fatigue, 29 (2007) 81.
[8] A. Risitano, G. Risitano, Int. J. Fatigue, 48 (2013) 214.
[9] C. E. Feltner, J. D. Morrow, Trans. ASME, Series D, J. Basic Eng., 83 (1961) 15.
[10] T. Boulanger, A. Chrysochoos, C. Mabru, A. Galtier, Int. J. Fatigue, 26 (2004) 221.
[11] J. L. Fan, X. L. Guo, V. Crupi, E. Guglielmino, C. W. Wu, Y. G. Zhao, Advanced Science Letters, 16 (2012) 305.
[12] E. H. Jordan, Exp. Mech., 25 (1985) 24.
[13] J. Gao, R. H. Wagoner Metall. Mater. Trans. A, 18 A (1987) 1001.
[14] A. Risitano, G. Risitano, C. Clienti, In: Proceedings of ICEM14, Poitiers (2010).
[15] A. Risitano, G. Risitano, Fatigue Fract. Eng. Mater. Struct., (2013) on-line, ISSN: 8756-758X.
[16] A. Risitano, Mechanical Design, first ed., CRC Press, New York, (2011).
[17] C. Clienti, G. Fargione, G. La Rosa, A. Risitano, G. Risitano, Eng. Fract. Mech., 77 (2010) 2158-2167.
[18] H. Neuber, Theory of notch stresses, Springer, Berlin, (1958).
[19] N. E. Frost, K. J. Marsh, L. P. Pook, Metal Fatigue, Oxford University Press, Oxford, (1974).
[20] R. A. Smith, K. J. Miller, Int. J Mech. Sci., 20 (1978) 201.
[21] J. C. Ting, F. V. Lawrence, Fatigue Fract. Eng. Mater. Struct., 16 (1993) 631.
[22] G. Meneghetti, M. Ricotta, D. Parolin, B. Atzori, In: Proceedings of MESO2012, Budapest, (2012).
[23] T. Boukharouba, T. Tamine, L. Nui, C. Chehimi, G. Pluvinage, Eng Fract Mech, 52 (1995) 503.
[24] M. L. Dunn, W. Suwito, S. J. Cunningham, Int. J. Solids Struct., 34 (1997) 3873.
[25] B. Atzori, P. Lazzarin, G. Meneghetti, Fatigue Fract. Eng. Mater. Struct., 26 (2003) 257.
[26] B. Atzori, G. Meneghetti, L. Susmel, Fatigue Fract. Eng. Mater. Struct., 28 (2005) 83.
[27] R. D. Henshell, K. G. Shaw, Int. J. Numer. Meth. Eng., 9 (1975) 495.
[28] A. Seweryn, Int. J. Solids Struct., 39 (2002) 4787.
[29] G. C. Sih, Int. J. Fract., 10 (1974) 305.
[30] P. Lazzarin, R. Tovo, Int. J. Fract., 78 (1996) 3.
[31] G. Glink, K.Molski Mater. Sci. Eng., 50 (1981) 93.
[32] P. Lazzarin, F. Berto, B. Atzori, Theor. Appl. Fract. Mec., 63–64 (2013) 32.
[33] P. Lazzarin, R. Zambardi, Fatigue Fract. Eng. Mater. Struct., 25 (2002) 917.
[34] F. J. Gómez, M. Elices, Int. J. Fract., 123 (2003) 163.
[35] P. Lazzarin, F. Berto, Int. J. Fract., 135 (2005) 161.
[36] F. J. Gomez, M. Elices, F. Berto, P. Lazzarin, Int. J. Fract., 145 (2007) 29.
[37] W. Nowacki, Thermoelasticity Pergamon Press, Oxford (1986).
[38] R. Giovannozzi, Costruzione di Macchine, Patron, Bologna, I (1951).
[39] F. Berto, P. Lazzarin, La Metallurgia Italiana, 3 (2005) 23.
[40] A. Risitano, D. Corallo, G. Risitano, A. Sirigu, In: Proceedings of XXXIX AIAS National Conference, (2010).
[41] N. Ranca, T. Palin-Luc, P. C. Paris, N. Saintier, Int. J. Fatigue (2013) on-line, DOI: 10.1016/j.ijfatigue.2013.04.012.

NOMENCLATURE

Symbol	Definition
σ	stress
σ_0	fatigue limit for R = -1 (limit stress above which some crystals are plasticised)
σ_i	minimum stress
σ_s	maximum stress
σ_u	ultimate stress
σ_p	plastic stress

$\sigma_{0.2}$	yield stress
ε	strain
ε_p	plastic strain
η	notch sensitivity
α_i	Stress concentration factor
α_{tT}	Stress concentration factor as ratio between ΔT_{max} e ΔT_{av} in total elastic phase
β_t	fatigue-stress concentration factor by mean of α_i and η
β_{ts}	ratio between material base fatigue limit and fatigue limit notched specimens
β_{tst}	ratio between σ corresponding T_0 for material base and T_0 for notched specimens
β_{tT}	ratio between ΔT_{max} e ΔT_{av} after total elastic phase
R	stress ratio
f	loading frequency
N	current number of cycles
ΔT_{max}	Maxima Temperature increment
ΔT_{av}	Average temperature increment
T	surface temperature
T_a	ambient temperature
T_0	"limit temperature" (corresponding to the end of the total thermo-elastic phase)
$\angle T°$	temperature increment of the hottest area
E	modulus of elasticity